

# WEIGHING THE ANCHOR IN CATEGORIZATION OF SOUND LEVEL

Elad Sagi<sup>1,2</sup> and Kenneth H. Norwich<sup>1,2,3</sup>

1 - Institute of Biomaterials and Biomedical Engineering, University of Toronto

2 - Department of Physiology and 3 - Department of Physics, University of Toronto

## ABSTRACT

Categorization of sound level requires that the subject classify the intensity of stimulus tones into appropriate response categories. Intensities are selected at random from a fixed stimulus range and stimulus-response pairs are tabulated into a stimulus-response matrix. "Anchor" or edge effects are well-recognized phenomena by which tones selected from the extremities of the stimulus range are classified with greater accuracy than tones in mid-range. Observation reveals that data in the center rows of a matrix follow a typical normal error distribution, while data in extreme rows follow a heavily skewed distribution with smaller variance. We propose that the distribution of responses along all rows of the stimulus-response matrix is described by a single, underlying normal density of constant variance. We develop the mathematical theory for extracting this constant underlying variance,  $\sigma^2$ , from an experimental "parent" matrix. A set consisting of all possible matrices (including the parent matrix) with core variance,  $\sigma^2$ , and containing the usual anchor phenomena, can then be generated at will. Using this core variance, we derive an expression for the transmitted information,  $I_T$ , that comprises a non-anchor and anchor contribution, whereby the size of the anchor effect may be quantified. Essentially, we provide a method for removing anchor effects and revealing the single core variance that represents, by hypothesis, the stimulus-response matrix.

## SOMMAIRE

Pour catégoriser le niveau sonore, le participant doit classer l'intensité des stimuli sonores selon des catégories de réponse adaptées. Les intensités sont choisies au hasard dans une étendue prédéterminée de stimuli et les couples stimulus-réponse sont reportés dans une matrice stimulus-réponse. Les « effets des points d'ancrage » sont des phénomènes connus selon lesquels les fréquences sonores appartenant aux extrémités de l'étendue de stimuli sont classées avec plus de précision que celles du milieu de l'étendue. Les données des rangées au milieu de la matrice sont réparties selon une courbe de Gauss classique, tandis que les données des rangées aux extrémités forment une distribution très asymétrique dont la variance est moins prononcée. Nous proposons que la répartition des réponses dans toutes les rangées de la matrice stimulus-réponse s'explique par la présence d'une courbe normale à variance constante. Nous élaborons la théorie mathématique visant à extraire cette variance constante sous-jacente,  $\sigma^2$ , d'une matrice « parentale » expérimentale. Une série composée de toutes les matrices possibles (y compris la matrice parentale), se caractérisant par une variance fondamentale,  $\sigma^2$ , et contenant les phénomènes classiques d'ancrage, peut alors être générée à volonté. En utilisant cette variance fondamentale, nous dérivons une expression pour l'information transmise,  $I_T$ , qui comprend un volet, tant ancré que non ancré, sur la base duquel l'ampleur de l'effet d'ancrage est quantifiable. Essentiellement, nous présentons une méthode visant à éliminer les effets d'ancrage et à révéler la variance fondamentale qui représente, selon l'hypothèse posée, la matrice stimulus-réponse.

## 1. INTRODUCTION

In tests of categorization of sound level, subjects are required to classify the intensity of tones into specific categories. For example, consider an experiment where a subject is presented with a tone, the intensity of which is selected randomly from a fixed range of 1 to 90 decibels (dB). This intensity range can be subdivided into 9 large categories of

10 dB width where 'category 1' equals 1-10 dB, 'category 2' equals 11-20 dB, and so on; or 30 small categories of 3 dB width where 'category 1' equals 1-3 dB, 'category 2' equals 4-6 dB, and so on. The number of categories used depends only on the requirements of the experimenter. The subject's task is to estimate the category to which the stimulus belongs to the best of his/her ability. More generally, the intensity of tones are randomly selected by the experimenter, typically using a uniform distribution, from a discrete set of stimulus

categories,  $X = \{X_1, \dots, X_m\}$ . Observers are required to classify each stimulus using a corresponding set of response categories,  $Y = \{Y_1, \dots, Y_m\}$ . Results are tabulated in the form of a stimulus-response or “confusion” matrix such that the element  $n_{jk}$  represents the number of times stimulus  $X_j$  was identified as response  $Y_k$ .

Illustrated in Figure 1 is a 10 x 10 stimulus-response matrix obtained from an experiment on stimulus categorization conducted in our laboratory using stimulus tones fixed at 1000 Hz and varying in intensity from 1 to 10 dB Hearing Level, i.e. decibels above a population threshold (dB HL). Each stimulus and response category is of width 1 dB. For example  $(X_5, Y_4) = 14$  means that the subject identified a 5 dB stimulus tone as a 4 dB tone 14 times out of the 45 times that this stimulus tone was given.

We consider here tones of a fixed frequency of 1000 Hz that vary only in intensity, from which we shall calculate Shannon’s mutual or transmitted information,  $I_t$ , by the methods of Garner and Hake (1951).

Adequate estimates of  $I_t$  require on the order of 10,000 trials, which, in the past has required pooling of data from several subjects. We have avoided pooling by extending data from a given participant using computer simulation. Wong and Norwich (1997) extended the work of Houtsma (1983) in developing such a simulator that permits estimation of  $I_t$  from limited data. Simulation is made possible because the distribution of responses in most rows of a confusion matrix has been observed to be Gaussian, with a constant row variance.

The simulator operates in the following way. Using a limited set of measured data, the row variance,  $\sigma^2$ , is estimated. Responses that are normally distributed with the measured variance,  $\sigma^2$ , are then computer generated by Monte Carlo techniques. The ‘simulated’ stimulus-response pair,  $(X_j, Y_k)$ , can then be compiled into a stimulus-response matrix and  $I_t$  can be measured. Continuing this process for an arbitrarily large number of trials provides an estimate of  $I_t$  that is based on a simulated stimulus-response matrix free from any small sample bias. The value of  $\sigma^2$  utilized by the simulator is estimated from a limited number of experimental trials conducted on a single subject. Converging estimates of  $\sigma^2$  require far fewer experimental trials than are required for overcoming the small sample bias in  $I_t$ . By way of illustration, the largest stimulus-response matrix obtained in our experiments is a 90 x 90 matrix corresponding to a stimulus range spanning 1 – 90 dB HL. Using our simulator it is easily verified that, whereas converging estimates of  $I_t$  require on the order of 50,000 simulated trials, less than 500 trials are required to obtain converging estimates of  $\sigma^2$ .

A drawback to the simulation approach as we had employed it is that apparent anchor effects were accounted for in only preliminary fashion. Although an observer’s responses to the mid-range intensities may follow normal distributions of common variance, the response distributions surrounding the more extreme intensities display heavy skewing or “anchoring”. That is, participants perform better in resolving intensities located at the extremes

	$Y_1$	$Y_2$	$Y_3$	$Y_4$	$Y_5$	$Y_6$	$Y_7$	$Y_8$	$Y_9$	$Y_{10}$	$X_i^{total}$
$X_1$	20	7	12	9	4	1	0	0	0	0	53
$X_2$	10	10	15	10	10	1	1	0	0	0	57
$X_3$	14	11	7	10	6	1	2	1	0	0	52
$X_4$	1	5	14	16	9	2	4	0	0	0	51
$X_5$	4	1	4	14	11	8	2	1	0	0	45
$X_6$	0	0	5	8	14	12	10	6	0	1	56
$X_7$	0	0	0	2	8	7	8	14	7	1	47
$X_8$	0	0	0	1	2	7	17	9	9	4	49
$X_9$	0	0	0	0	3	4	11	18	11	4	51
$X_{10}$	0	0	0	1	1	0	2	4	18	13	39
$Y_k^{total}$	49	34	57	71	68	43	57	53	45	23	500

**Figure 1: A 10 x 10 stimulus-response matrix conducted over a stimulus range of 1 - 10 dB HL. Note normal distribution about main diagonal across middle rows.**

of the stimulus range, as if their responses were intrinsically anchored.

This can be seen in Figure 1, especially along row 1 and row 10 where the subject's responses are heavily skewed, or anchored, to the sides of the matrix. Please notice that responses along the middle rows tend to follow a normal distribution about the main diagonal, while responses along the extreme rows are skewed due to anchor effects. Since the reduced variances of these extreme distributions would be incorporated into a sample estimate for  $\sigma$ , the accuracy of the resulting information estimates would be affected. We propose that one can remove the skewing and assign a common normal distribution to all the rows.

In this paper we are interested in developing a means of estimating  $\sigma^2$  that is not affected by the anchoring process. A model is developed where  $\sigma^2$ , the 'anchor-free' variance underlying the stimulus-response matrix, is extracted from a measure of the average row variance of this matrix,  $\sigma^2_{eff}$  which contains the anchor effect. This model is used to obtain more accurate estimates of the transmitted information as measured from the stimulus-response matrix. Finally, an expression for the transmitted information is derived that decomposes into a sum of two parts, a non-anchor and an anchor contribution, whereby the magnitude of the anchor effect may be measured.

## 2. A CONSTANT VARIANCE (CV) MODEL FOR THE STIMULUS-RESPONSE MATRIX

It is assumed that there is a single, unique normal distribution governing responses in each row of the matrix, which is perturbed by the "anchor" process. Let  $\sigma^2$  be the "constant variance" of this normal distribution and let  $\sigma^2_{eff}$  represent the arithmetic mean of variances across all rows of the stimulus-response matrix, including the extreme distributions. If  $\sigma$  underlies all responses of the stimulus-response matrix, it should be possible to relate  $\sigma^2_{eff}$  to  $\sigma$ .

Finding a relationship between  $\sigma^2_{eff}$  and  $\sigma$  requires a model of the row distributions. For ease in calculation, the set of discrete responses,  $Y$ , will be represented by the continuous random variable,  $y$ , and the set of discrete stimuli,  $X$ , will be represented by the continuous random variable,  $x$ . One should note the necessary correction of the form  $y = Y_k - 0.5$  and  $x = X_j - 0.5$  when transforming from the continuous domain to the discrete domain (cf Snedecor, 1980, p118).

We represent distributions along any row of the stimulus-response matrix as a conditional probability of response  $y$  given a value of  $x$ . This distribution,  $p^*(y|x)$  is a continuous normal distribution with variance  $\sigma^2$ :

$$p^*(y|x) = \frac{1}{\sqrt{2\pi\sigma^2}} \exp\left[-\frac{1}{2}\left(\frac{y-x}{\sigma}\right)^2\right] \quad (1)$$

$p^*(y|x)$  is, however, unbounded in  $y$  such that  $y \in (-\infty, \infty)$ .

To conform to the boundaries of the matrix more realistically, one can confine  $p^*(y|x)$  to the width of the matrix; namely, define  $y$  such that  $y \in [0, R]$  (which is the continuous analogue of  $Y \in \{1, 2, \dots, R\}$ ). If we now integrate over the space of  $y$ ,

$$\begin{aligned} \int_0^R p^*(y|x) dy &= \int_0^R \frac{1}{\sqrt{2\pi\sigma^2}} \exp\left[-\frac{1}{2}\left(\frac{y-x}{\sigma}\right)^2\right] dy \\ &= \frac{1}{2} \left[ \operatorname{erf}\left(\frac{R-x}{\sigma\sqrt{2}}\right) + \operatorname{erf}\left(\frac{x}{\sigma\sqrt{2}}\right) \right] \\ &= C(x). \end{aligned}$$

Dividing  $p^*(y|x)$  by  $C(x)$  renormalizes Eq. (1) over the range, giving an expression,  $p(y|x)$ , for the row distributions as follows:

$$\begin{aligned} p(y|x) &= \frac{1}{C(x)\sqrt{2\pi\sigma^2}} \exp\left[-\frac{1}{2}\left(\frac{y-x}{\sigma}\right)^2\right] \\ C(x) &= \frac{1}{2} \left[ \operatorname{erf}\left(\frac{R-x}{\sigma\sqrt{2}}\right) + \operatorname{erf}\left(\frac{x}{\sigma\sqrt{2}}\right) \right] \\ x, y &\in [0, R] \end{aligned} \quad (2)$$

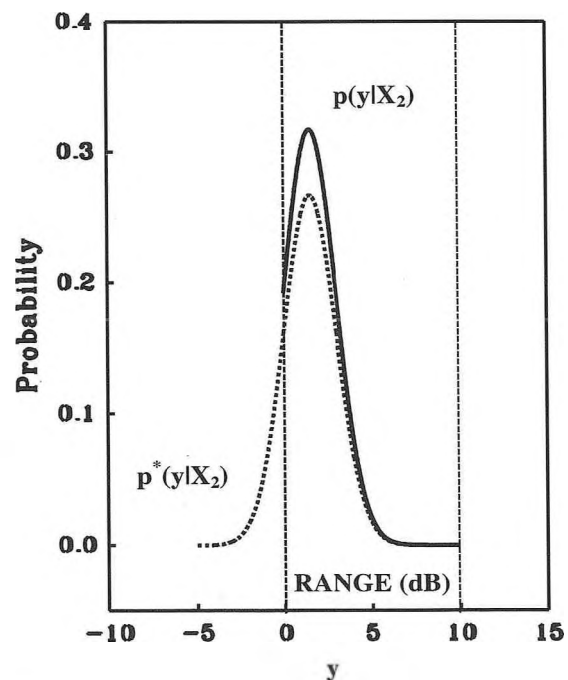


Figure 2: A continuous normal distribution, whose mean lies at the center of the second column of a 10 x 10 matrix, is renormalized over the continuous range [0, 10] dB.

This procedure is outlined graphically in Figure 2 where we consider the second row ( $X_2$ ) of a typical 10 x 10 confusion matrix over a range 1 – 10 dB. The dashed curve represents a continuous, normal distribution,  $p^*(y|X_2)$ , of variance  $\sigma^2$  centered over the second column ( $y = 1.5$ ). The solid curve is the distribution,  $p(y|X_2)$ , that results from renormalizing  $p^*(y|X_2)$  over a fixed range [0, 10] dB. This range is the continuous analogue of the discrete categorical range {1, ..., 10}. As a result of confining  $p^*(y|X_2)$  to the stimulus range,  $p(y|X_2)$  is skewed and of smaller variance.

The renormalized distribution,  $p(y|x)$ , is now sufficient to describe the distribution of responses along the rows of a stimulus-response matrix as seen in Figure 3. The resulting set of distributions are all related to the same underlying normal distribution of constant variance,  $\sigma^2$ . We observe that the distributions skew as the mean approaches the edges.

Renormalizing  $p^*(y|x)$  (unskewed) over the range and shifting the means appropriately gives rise to the set of skewed distributions,  $p(y|X_j)$  ( $j = 1, \dots, R$ ). Since  $\sigma^2$  is the variance belonging to  $p^*(y|x)$  and  $\sigma_{eff}^2$  is the average variance of the  $p(y|X_j)$ 's, we should expect that  $\sigma_{eff}^2 \leq \sigma^2$ .

To evaluate  $\sigma^2$  as a function of  $\sigma_{eff}^2$  we first evaluate the variance of each row. That is,

$$\text{var}[p(y|x)] = \langle y^2 \rangle - \langle y \rangle^2$$

where  $\langle y \rangle$  and  $\langle y^2 \rangle$  are the first and second moments of

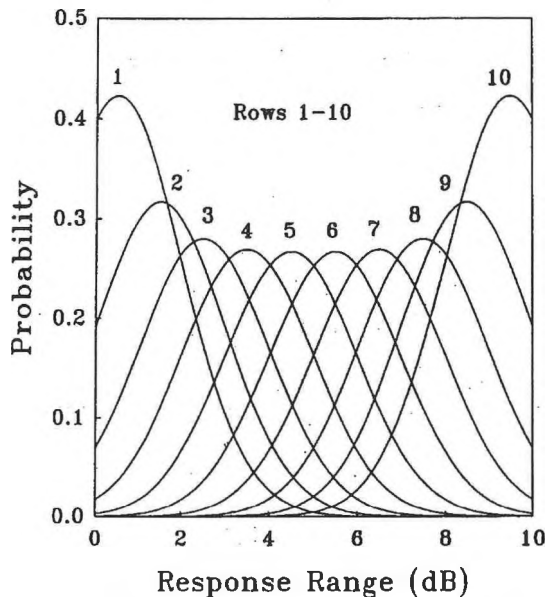


Figure 3: The process of renormalizing  $p^*(y|X_j)$ , as displayed in Figure 2, for all stimulus categories  $X_j$  ( $j = 1, \dots, 10$ ) over the fixed range [0, 10] dB.

$p(y|x)$  respectively. We have defined  $\sigma_{eff}^2$  as the arithmetic mean of the row variances, or

$$\sigma_{eff}^2 = \frac{1}{R} \int_0^R \text{var}[p(y|x)] dx.$$

In the appendix, part I, it is shown that for  $R \gg \sigma$ ,

$$\sigma_{eff}^2 = \sigma^2 - \frac{4}{R\sqrt{2\pi}} \sigma^3. \quad (3)$$

Eq. (3) allows us to convert the average variance of the skewed distributions in the stimulus-response matrix to the variance of the unskewed normal distribution that underlies responses. That is, Eq. (3) can be used to extract the underlying variance,  $\sigma^2$ , from the average row variance,  $\sigma_{eff}^2$ , measured from experiment. We observe that  $\sigma_{eff}^2 \leq \sigma^2$ , as expected.

### 3. APPLICATION OF CV MODEL TO EXPERIMENT

We shall now simulate the matrix in Figure 1 using Eq. (3). Measuring the average row variance from the matrix gives  $s_{eff}^2 = 2.21$ . The notation  $s_{eff}^2$  is used to describe the sample mean row variance corresponding to  $\sigma_{eff}^2$ , the actual mean row variance. Similarly,  $s^2$  is the sample estimate corresponding to  $\sigma^2$ . Substituting ( $s_{eff}^2$  for  $\sigma_{eff}^2$ ) into Eq. (3) and solving gives  $s^2 = 3.07$ . This value is now used as an input into the simulator.

In Figure 4, the dashed curve depicts information calculated progressively from the stimulus-response matrix displayed in Figure 1 as the matrix fills by increasing numbers of experimental trials. The solid curve represents information calculated progressively from an average of 20 Monte Carlo simulations. Two types of input were used for simulation. The first was the arithmetic mean row variance calculated directly from the matrix in Figure 1; i.e.  $s_{eff}^2 = 2.21$  (top panel). The second was the corrected variance obtained by substituting  $s_{eff}^2$  (for  $\sigma_{eff}^2$ ) into Eq. (3) to give  $s^2 = 3.07$  (bottom panel). Notice how, after 500 trials, the simulator that implements Eq. (3) to obtain  $s^2 = 3.07$  as an input conforms more closely to the experimental curve, thus improving upon the method of overcoming small sample bias developed by Wong and Norwich (1997). Furthermore, the close correspondence between experiment and simulation in Figure 4 using the anchor free estimate of  $\sigma^2$  attests to the validity of the constant variance assumption.

The procedure in our example can be generalized. For

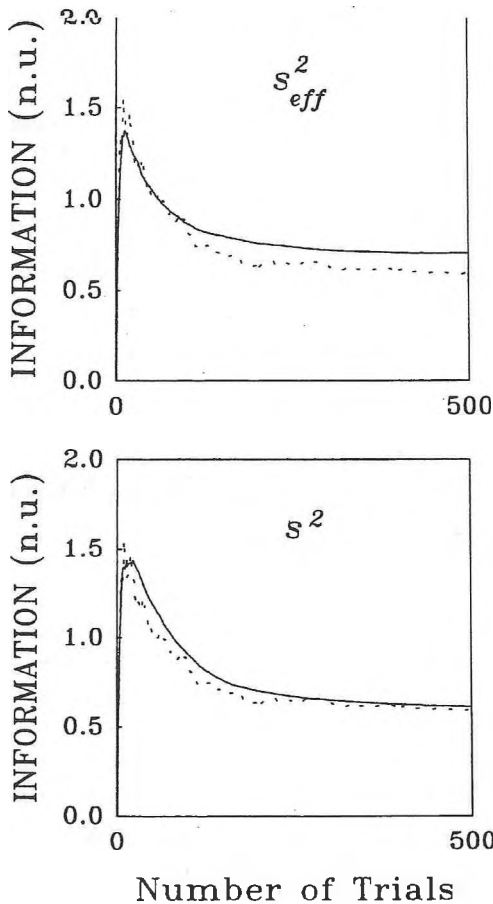


**Figure 4: Comparison of two inputs for simulation, upper and lower panels. Information calculated from experiment (dashed curve) and simulation (solid curve) as stimulus-response matrix fills by increasing number of trials.**

any experimentally determined stimulus-response matrix, measure the average row sample variance,  $s_{eff}^2$ . “Unwrap” this measure (or “weigh” the anchor) using Eq. (3) to obtain the anchor-free estimate,  $s^2$ , of the response error underlying the matrix. Simulate using  $s^2$  to obtain an estimate for information,  $I(N)$ , to any desired number of trials.

One should note that averaging simulations gives a stronger estimate of the expected value of information  $\langle I(N) \rangle$  corresponding to the underlying response error,  $\sigma$ .  $I(N)$  resulting from a single simulation can be considered as a single experiment. The corresponding expectation,  $\langle I(N) \rangle$  would represent a long term average over many experiments and has a one-to-one correspondence with  $\sigma$ . The characteristic shape of  $\langle I(N) \rangle$  as depicted in Figure 4 has been discussed by Norwich, Wong and Sagi (1998). One should note that for  $N \rightarrow \infty$ ,  $I(N) \rightarrow I_t$ . That is, after a sufficient number of trials, the small sample bias in the information estimate,  $I(N)$ , is overcome and one obtains the information transmitted to the subject,  $I_t$ .

#### 4. BYPASSING SIMULATION BY APPROXIMATION: THE ASYMPTOTIC INFORMATION

As mentioned, the original purpose for simulation was to overcome the small sample bias in calculated information,  $I(N)$ , which approaches transmitted information,  $I_t$ , only after a significant number of trials. One of the advantages of the CV model is that it provides a trial-independent, *a priori* description of the row distributions found in the stimulus-response matrix; namely,  $p(y|x)$ , which can be substituted into the equation that describes  $I_t$  (Garner and Hake, 1951).

$$I_t \equiv I(Y|X) = H(Y) - H(Y|X) \\ = -\sum_{k=1}^R p(y_k) \log p(y_k) + \sum_{j=1}^R \sum_{k=1}^R p(x_j) p(y_k|x_j) \log p(y_k|x_j) \quad (4)$$

This equation is independent of  $N$  and describes  $I_t$  exactly, but is too difficult to handle analytically. We can, however make some approximations. First, let us transfer from the discrete realm to the continuous, thereby converting sums into integrals. This procedure is analogous to considering infinitesimally small category widths. The increase in  $I_t$  due to an increasing number of categories is a well known phenomenon (Miller, 1956). This increase, however, is bounded. That is, for a large enough number of categories,  $I_t$  approaches a constant value, i.e. the channel capacity for that stimulus range.

By way of example, the channel capacity for a stimulus range spanning 90 dB is reached after about 30 categories, i.e. each category having a width of 3 dB. Similarly, the channel capacity for a stimulus range spanning 30 dB is reached after about 10 categories. Of course, the channel capacity for the 90 dB stimulus range is larger than that for the stimulus range of 30 dB. In our experiments, we use categories of 1 dB width, which is the same as requiring that the number of categories equals the discrete stimulus range, i.e.  $m = R$  dB. Since, using this many categories, the transmitted information has reached channel capacity, we therefore make the conjecture that increasing the number of categories from  $m = R$  dB to  $m \rightarrow \infty$  in Eq. (4) has little or no effect on  $I_t$  (Sagi, Wong and Norwich, 2001).

Hence,

$$I_t = -\int_0^R p(y) \log p(y) dy + \int_0^R \int_0^R p(x) p(y|x) \log p(y|x) dy dx$$

Symmetry in a stimulus-response matrix would imply that  $p(y) = p(x) = 1/R$ :

$$I_t = \log R + \frac{1}{R} \int_0^R \int_0^R p(y|x) \log p(y|x) dy dx$$

Using the expression for the row distributions in Eq. (2), the integral of the rightmost term can be expanded as shown in the appendix, part II. The transmitted information in natural units now becomes

$$I_t = \ln R - \frac{1}{2} \ln(2\pi e \sigma^2) - \frac{1}{R} \int_0^R \left( \ln C(x) + \frac{\sigma^2}{2C(x)} \frac{d^2 C(x)}{dx^2} \right) dx$$

The rightmost term can be defined as follows:

$$\Phi(R, \sigma) = -\frac{1}{R} \int_0^R \left( \ln C(x) + \frac{\sigma^2}{2C(x)} \frac{d^2 C(x)}{dx^2} \right) dx$$

$$C(x) = \frac{1}{2} \left[ \operatorname{erf} \left( \frac{R-x}{\sigma\sqrt{2}} \right) + \operatorname{erf} \left( \frac{x}{\sigma\sqrt{2}} \right) \right] \quad (5)$$

and the information transmitted to the subject in natural units can be expressed as

$$I_t = \ln R - \frac{1}{2} \ln(2\pi e \sigma^2) + \Phi(R, \sigma) \quad (6)$$

Please note that in Eq. (5),  $\Phi(R, \sigma) \geq 0$  and must be evaluated numerically, but vanishes for large  $R$ . One can consider  $\Phi(R, \sigma)$  as an information gain due to the presence of edges. Notice how, in this model, no assumptions were necessary regarding mechanisms for anchoring. Instead, the anchor effect comes about naturally from the boundary condition  $y \in [0, R]$ .

If we drop  $\Phi(R, \sigma)$ , Eq. (6) becomes

$$I_t^* = \ln R - \frac{1}{2} \ln(2\pi e \sigma^2) \quad (7)$$

This expression compares well with that derived in Wong and Norwich (1997) where transmitted information was approximated without the anchor effect. A similar expression was also suggested by Baird (1984). Hence, it is possible to describe  $I_t$  in terms of a non-anchor contribution and an anchor contribution, or

$$I_t = I_t^* + \Phi(R, \sigma) \quad (8)$$

Data in Table 1 demonstrate the correspondence between the transmitted information,  $I_t$ , calculated from Eq. (6); the transmitted information independent of anchor effects,  $I_t^*$ , calculated from Eq. (7); and  $I_t^{sim}$ , the value of transmitted information obtained from the simulator. All information measurements were made in natural units (n.u.). For estimates of information using the simulator, 100,000 trials were used to overcome any small sample bias. Also, 20 runs are averaged for each simulation to ensure the simulator approx-

imates  $\langle I(N) \rangle$ . All information measures make use of the subject's estimated error of response,  $s$  (for  $\sigma$ ), for a given range. This estimate was "unwrapped" from  $s_{eff}$  (for  $\sigma_{eff}$ ), obtained experimentally from subject "W" over several ranges, using Equation (3). The information gain due to the presence of edges is expressed in terms of  $\% \Phi$ , defined below in Eq. (9).

Please notice in Table 1 the correspondence between  $I_t$  and  $I_t^{sim}$ . That is, Eq. (6) is sufficient to describe the results of simulations over large trials. Furthermore, the term  $\Phi(R, \sigma)$  allows us to quantify the added contribution of edge effects to  $I_t$ . Hereafter, all estimates of  $I_t$  will be obtained from Eq. (6).

## 5. EXPERIMENTS ON STIMULUS CATEGORIZATION

Experiments on categorization of intensities of auditory stimuli were conducted over several ranges of stimuli (Norwich et al, 1998). Stimulus tones of 1000 Hz and 1.5 s duration were presented binaurally through headphones to 5 participants. Each categorization experiment was conducted over a fixed stimulus range using 500 experimental trials. For each stimulus range, the number of categories equals the discrete range, or  $m = R$  dB, and  $s_{eff}^2$  was measured from the resulting stimulus-response matrix. For each participant,  $s^2$  was obtained from  $s_{eff}^2$  using Eq. (3) above.

Subsequently,  $s^2$  was used to calculate  $I_t$  and  $\Phi$  for each subject and each stimulus range using Eq. (6). The results are compiled in Table 2. Transmitted information ( $I_t$ ) increases with increasing stimulus range in accordance with the findings of previous investigators (Norwich et. al., 1998). Using Eq. (6) and Eq. (7) of the constant variance model, we are now able to quantify the percent contribution of the edge effect to the transmitted information,  $I_t$ , expressed as  $\% \Phi$ , calculated from

$$\% \Phi = 100 \frac{I_t - I_t^*}{I_t} \quad (9)$$

We observe that the edge or anchor effects predominate at smaller ranges and decrease with increasing stimulus range.

## 6. DISCUSSION AND CONCLUSION

We have presented a means by which anchor effects can be removed from a stimulus-response matrix. A constant variance model of the stimulus-response matrix was utilized. The primary assumption of the model is that the distribution

Range (dB)	$s_{eff}$ (dB)	$s$ (dB)	$I_t^{sim}$ (n.u.)	$I_t$ (n.u.)	$I_t^*$ (n.u.)	% $\Phi$
1 - 10	1.49	1.75	0.557	0.563	0.324	42
1 - 30	2.50	2.71	1.110	1.107	0.985	11
1 - 50	3.72	3.99	1.224	1.215	1.109	8.7
1 - 70	4.41	4.66	1.391	1.376	1.291	6.2
1 - 90	5.58	5.90	1.427	1.391	1.306	6.1

Table 1: Data from subject "W".  $s_{eff}$  obtained from experiment over given range.  $s$  obtained from  $s_{eff}$  using Eq. (3).  $s$  used to measure  $I_t^{sim}$  from simulation (see text),  $I_t$  from Eq. (6), and  $I_t^*$  from Eq. (7). % $\Phi$  from Eq. (9).

Information in natural units (n.u.).

Range (dB)	Subject "C"		Subject "E"		Subject "J"		Subject "R"		Subject "W"	
	$I_t$ (n.u.)	% $\Phi$								
1-10	0.841	20	0.632	35	0.595	39	0.790	22	0.563	42
1-30	1.086	11	1.125	10	0.979	14	1.208	8.7	1.107	11
1-50	-	-	1.226	8.5	1.049	12	-	-	1.215	8.7
1-70	-	-	-	-	1.232	8.4	-	-	1.376	6.2
1-90	1.252	8.1	1.432	8.1	1.482	5.2	1.499	5.0	1.391	6.1

Table 2: Percent contribution of the edge effect, % $\Phi$  (Eq. (9)), to the transmitted information,  $I_t$  (Eq. (6)) in natural units (n.u.), measured over several stimulus ranges for 5 subjects.

of responses along each row of the matrix, including the extreme intensities of the stimulus range, can be described by a single underlying normal density of constant variance,  $\sigma^2$ .

Although stimulus categorization experiments were performed with a limited number of experimental trials, accurate estimates of  $I_t$  are obtainable for each participant from the resulting stimulus-response matrix through Monte Carlo

simulation. Using a single input value for the subject's response error,  $\sigma^2$ , pseudo-stimulus-response pairs are generated for an arbitrarily large number of trials and the resulting information is calculated from the simulated stimulus-response matrix. In this way, small sample bias is minimized or eliminated.

The single input value,  $\sigma$ , can be measured from the experimentally obtained stimulus-response matrix in the form of an average row variance,  $\sigma_{eff}^2$ . This measure is, however, distorted or anchored by edge effects due to stimuli at the extremities of the stimulus range. The constant variance model removes the anchor, replacing  $\sigma_{eff}^2$  by the more accurate  $\sigma^2$ . This process is described qualitatively in Figure 5 where the process of "weighing the anchor in stimulus categorization" is summarized. Consider an experiment in stimulus categorization conducted over a sufficiently large number of trials. We can measure a subject's response error by taking an arithmetic mean of the variances across all the rows of the resulting matrix, to estimate  $\sigma_{eff}^2$ . This measure is anchored due to stimuli at the extremities of the stimulus range. The anchor effect can be removed (or "weighed") by substituting  $\sigma_{eff}^2$  into Eq. (3) of the constant variance model to obtain an estimator of  $\sigma^2$ . If we now utilize  $\sigma^2$  as input for simulation, we find, after a sufficiently

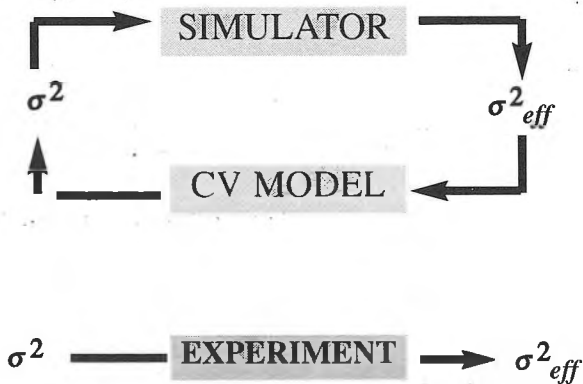


Figure 5: Using  $\sigma_{eff}^2$  measured from experiment, the CV model (Eq. 3) provides us with  $\sigma^2$  (anchor-free) as an input to the simulator, in turn, giving rise to the same  $\sigma_{eff}^2$  as an output: a kind of "Koch cycle".

large number of simulated trials, that the mean row variance of the resulting simulated stimulus-response matrix is equal to  $\sigma^2_{eff}$ , the value originally measured from experiment. Inputting  $\sigma^2$  into the simulator gives rise to  $\sigma^2_{eff}$  in the resulting simulated stimulus-response matrix. The constant variance model lets us estimate the value of  $\sigma^2$  that originally gave rise to  $\sigma^2_{eff}$ .

The process of beginning with  $\sigma^2_{eff}$  from experiments on the “outside world”, passing it through the model and simulator, and then retrieving  $\sigma^2_{eff}$  back into the outside world, is strangely reminiscent of the postulates (criteria) of microbiologist Robert Koch (see, for example, Dorland’s Illustrated Medical Dictionary, 28<sup>th</sup> Edition). That is, our ability to extract an otherwise hidden parameter, i.e.  $\sigma^2$ , depends on the extent to which we are able to reproduce the observable,  $\sigma^2_{eff}$ .

Our ability to recreate the experimentally observed stimulus-response matrix is best demonstrated using the calculated information,  $I(N)$ , as in Figure 4. Using  $\sigma^2$  that is free from the anchor effect as the single input parameter to the simulator, both the small sample bias in  $I(N)$  and its subsequent approach to  $I_t$  are accounted for. In this way, we have a theoretical ‘handle’ on what may not be just a statistical bias, but a description of the progressive acquisition of auditory information.

Furthermore, confining the underlying normal distribution of constant variance,  $\sigma^2$ , to the stimulus range and then renormalizing this distribution over that range provides us with an *a priori* description of the probability distribution for any given row. This leads to a trial-independent expression for the transmitted information, obviating the need for simulation. The expression for  $I_t$  decomposes into a sum of two components, the first independent of, and the second dependent upon the anchor effects. Hence, we are truly able to “weigh” the contribution of the anchor effect to the transmitted information that arises somewhat as an artifact from the boundary conditions of the experiment.

The primary utility of the constant variance assumption is that an experiment on categorization of sound level over a fixed stimulus range becomes completely determined by a single parameter, i.e.  $\sigma^2$ . As demonstrated in Table 2,  $\sigma^2$  increases as the stimulus range is increased. Recently, we have demonstrated that the rate of increase of  $\sigma^2$  with stimulus range mirrors the rate of increase of psychophysical loudness with stimulus intensity. In this way,  $\sigma^2$  becomes a rather ‘objective’ representation of loudness (Norwich and Sagi, 2002, in press).

Although the focus of our experiments was on categorization, or absolute identification of sound level, the theory

outlined herein could be applied to categorization, or absolute identification of other dimensions such as pitch, spatial perception, etc.

## 7. ACKNOWLEDGMENTS

This research has been supported by an operating grant from NSERC, the Natural Sciences and Engineering Research Council of Canada. Elad Sagi has been supported by an NSERC Scholarship.

## 8. REFERENCES

- Baird, J. C. (1984). Information theory and information processing. *Information Processing and Management*, 20, 373-381.
- Garner, W. R. and Hake, H. W. (1951). The amount of information in absolute judgments. *Psychological Review*, 58, 446-459.
- Houtsma, A. J. M. (1983). Estimation of mutual information from limited experimental data, *Journal of the Acoustical Society of America*, 74, 1626-1629.
- Miller, G. A. (1956). The magical number seven plus or minus two: Some limits on our capacity for processing information. *Psychological Review*, 63, 81-97.
- Norwich, K. H., Wong, W. and Sagi, E. (1998). Range as a factor in determining the information of loudness judgments: Overcoming small sample bias. *Canadian Journal of Experimental Psychology*, 52, 63-70.
- Norwich, K. H. and Sagi, E. (2002). Deriving the loudness exponent from categorical judgments. *Perception and Psychophysics*, in press.
- Sagi, E. (1998). Absolute identification of loudness: Theory and Experiment. *M.Sc. Thesis*, University of Toronto.
- Sagi, E., Wong, W. and Norwich, K. H. (2001). Mathematical studies of the information in the stimulus-response matrix. *Journal of Mathematical Psychology*, 45, 99-114.
- Snedecor, G. W. and Cochran, W. G. (1980). *Statistical Methods*, 7<sup>th</sup> ed. (Ames, Iowa), The Iowa State University Press.
- Wong, W. and Norwich, K. H. (1997). Simulation of human sensory performance. *BioSystems*. 43, 189-197.

## APPENDIX

### (I) $\sigma^2_{eff}$ as a Function of $\sigma^2$

To obtain  $\sigma^2_{eff}$  as a function of  $\sigma^2$ , we require the first two moments of  $p(y|x)$ ; namely  $\langle y \rangle$  and  $\langle y^2 \rangle$ .

$$\begin{aligned} \langle y \rangle &= \int_0^R yp(y|x)dy \\ &= \int_0^R \frac{y}{C(x)\sqrt{2\pi\sigma^2}} \exp\left[-\frac{1}{2}\left(\frac{y-x}{\sigma}\right)^2\right] dy \end{aligned}$$

Employing the following substitution:

$$\begin{aligned} t &= \frac{y-x}{\sqrt{2}\sigma} \\ y &= \sqrt{2}\sigma t + x \end{aligned}$$

we obtain

$$\begin{aligned} \text{var}[p(y|x)] &= \langle y^2 \rangle - \langle y \rangle^2 \\ &= 2\sigma^2 \left( \langle t^2 \rangle - \langle t \rangle^2 \right) \end{aligned}$$

Making the necessary substitutions,

$$\begin{aligned} \langle t \rangle &= \int_{\frac{-x}{\sqrt{2}\sigma}}^{\frac{R-x}{\sqrt{2}\sigma}} \frac{t \exp(-t^2)}{C(x)\sqrt{\pi}} dt \\ &= \frac{\sigma}{C(x)\sqrt{2}} \frac{\exp\left(-\frac{1}{2}\left(\frac{x}{\sigma}\right)^2\right) - \exp\left(-\frac{1}{2}\left(\frac{R-x}{\sigma}\right)^2\right)}{\sqrt{2\pi\sigma^2}} \end{aligned}$$

This equation can be conveniently expressed in a shorthand using the normalizing factor  $C(x)$ :

$$\begin{aligned} \langle t \rangle &= \frac{\sigma}{C(x)\sqrt{2}} \frac{dC(x)}{dx} \\ C(x) &= \frac{1}{2} \text{erf}\left(\frac{R-x}{\sqrt{2}\sigma}\right) + \frac{1}{2} \text{erf}\left(\frac{x}{\sqrt{2}\sigma}\right) \end{aligned}$$

One can take a similar approach for the second moment:

$$\begin{aligned} \langle t^2 \rangle &= \int_{\frac{-x}{\sqrt{2}\sigma}}^{\frac{R-x}{\sqrt{2}\sigma}} \frac{t^2 \exp(-t^2)}{C(x)\sqrt{\pi}} dt \\ &= \frac{1}{C(x)2\sqrt{\pi}} \left( -t \exp(-t^2) \Big|_{\frac{-x}{\sqrt{2}\sigma}}^{\frac{R-x}{\sqrt{2}\sigma}} + \frac{1}{2} \right) \end{aligned}$$

Using the same shorthand above,

$$\langle t^2 \rangle = \frac{\sigma^2}{2C(x)} \frac{d^2C(x)}{dx^2} + \frac{1}{2}$$

We now can express the variance of any row distribution as a function of its mean:

$$\begin{aligned} \text{var}[p(y|x)] &= 2\sigma^2 \left( \langle t^2 \rangle - \langle t \rangle^2 \right) \\ &= \frac{\sigma^4}{C(x)} \frac{d^2C(x)}{dx^2} + \sigma^2 - \frac{\sigma^4}{(C(x))^2} \left( \frac{dC(x)}{dx} \right)^2 \end{aligned}$$

One should note that

$$\frac{d}{dx} \left( \frac{1}{C(x)} \frac{dC(x)}{dx} \right) = \frac{1}{C(x)} \frac{d^2C(x)}{dx^2} - \frac{1}{(C(x))^2} \left( \frac{dC(x)}{dx} \right)^2$$

so the variance of any row distribution becomes:

$$\text{var}[p(y|x)] = \sigma^4 \frac{d}{dx} \left( \frac{1}{C(x)} \frac{dC(x)}{dx} \right) + \sigma^2$$

The latter is still a complicated expression and difficult to work with. However, if we measure the average row variance over the mean, we can obtain an expression for  $\sigma^2_{eff}$ . In the discrete case, taking an arithmetic mean for the row variance simply involves adding the variances of rows 1 to  $R$  and dividing by the range,  $R$ . Deriving a closed expression for this using  $\text{var}[p(y|x)]$  above would be quite difficult. It is possible, however, to consider jumping from the discrete case to the continuous case over the mean  $x$ . Specifically,  $\sigma^2_{eff}$  in the continuous case takes the form:

$$\begin{aligned} \sigma^2_{eff} &= \frac{1}{R} \int_0^R \text{var}[p(y|x)] dx \\ &= \frac{1}{R} \int_0^R \left[ \sigma^4 \frac{d}{dx} \left( \frac{1}{C(x)} \frac{dC(x)}{dx} \right) + \sigma^2 \right] dx \end{aligned}$$

It is easily verified that for  $R \gg \sigma$ ,

$$\begin{aligned} \left( \frac{1}{C(x)} \frac{dC(x)}{dx} \right)_0^R &= \frac{\sqrt{2}}{\sigma} \left( \frac{\frac{2}{\sqrt{\pi}} \exp\left[-\left(\frac{R}{\sqrt{2}\sigma}\right)^2\right] - \frac{2}{\sqrt{\pi}}}{\text{erf}\left(\frac{R}{\sqrt{2}\sigma}\right)} \right) \\ &\equiv -\frac{4}{\sqrt{2\pi\sigma^2}} \end{aligned}$$

So to a strong approximation,

$$\sigma_{eff}^2 = \sigma^2 - \frac{4}{R\sqrt{2\pi}}\sigma^3$$

which is Eq. (3).

## (II) Asymptotic Approximation

We would now like to evaluate the integral:

$$H(Y|X) = -\frac{1}{R} \int_0^R \int_0^R p(y|x) \ln p(y|x) dy dx,$$

where  $p(y|x)$  is defined in Eq. (2).

$$H(Y|X) = -\frac{1}{R} \int_0^R \int_0^R \left[ \frac{e^{-\frac{1}{2}\left(\frac{y-x}{\sigma}\right)^2}}{C(x)\sqrt{2\pi\sigma^2}} \right] \ln \left[ \frac{e^{-\frac{1}{2}\left(\frac{y-x}{\sigma}\right)^2}}{C(x)\sqrt{2\pi\sigma^2}} \right] dy dx$$

After some simplification

$$H(Y|X) = \frac{1}{R} \int_0^R \langle t^2 \rangle dx + \frac{1}{R} \int_0^R \ln(C(x)) dx + \frac{1}{2} \ln(2\pi\sigma^2)$$

where  $\langle t^2 \rangle$  is described previously in the appendix. The full expression therefore becomes

$$H(Y|X) = \frac{1}{R} \int_0^R \left( \frac{\sigma^2}{2C(x)} \frac{d^2C(x)}{dx^2} + \frac{1}{2} \right) dx + \frac{1}{R} \int_0^R \ln C(x) dx + \frac{1}{2} \ln(2\pi\sigma^2)$$

or finally,

$$H(Y|X) = \frac{1}{2} \ln(2\pi\sigma^2) + \frac{1}{R} \int_0^R \left( \frac{\sigma^2}{2C(x)} \frac{d^2C(x)}{dx^2} + \ln C(x) \right) dx$$

as used in Eq. (5).

When it's *versatile,*  
**reliable,** accurate  
*and* easy to use...



...you GO with it.

The new Norsonic 118 puts all the power you need right in the palm of your hand. This all-digital, modular sound level meter has an extensive set of functions available now — and the capacity to grow as your needs demand:

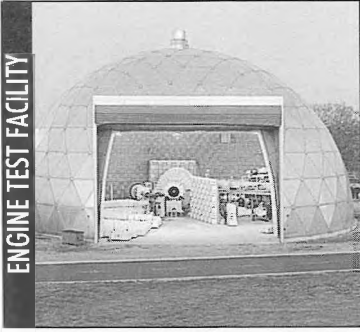
- Octave or 1/3-octave band RTA • Frequency range of 6.3–20kHz
- High resolution, backlit display • 120 dB dynamic range in 1/3 octave bands.
- Up to 2.5 million sound level data stored • High speed data transfer (to 115k baud).
- Real time frequency analysis in octave and 1/3 octave bands with extended range.
- Synchro measurements with real time clock • Simultaneous time constants.
- Sound power calculations per ISO 3744.

# Scantek

Sound and vibration  
instrumentation and engineering

7060 Oakland Mills Rd., Suite L, Columbia, MD 21046  
Tel: 410.290.7726 • Fax: 410.290.9167

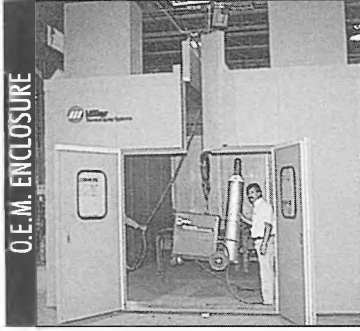
Go to: [www.scantekinc.com](http://www.scantekinc.com) or [info@scantekinc.com](mailto:info@scantekinc.com)



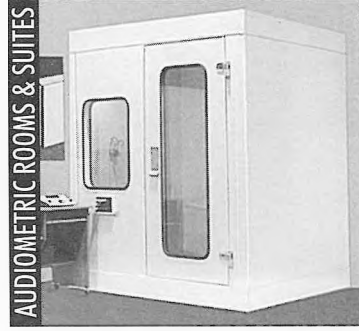
ENGINE TEST FACILITY



ECKOUSTIC FUNCTIONAL PANELS

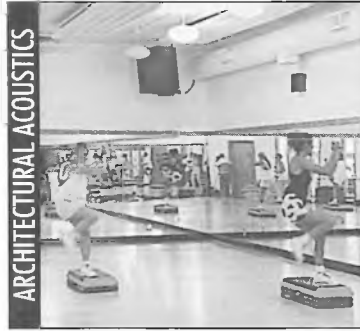


O.E.M. ENCLOSURE

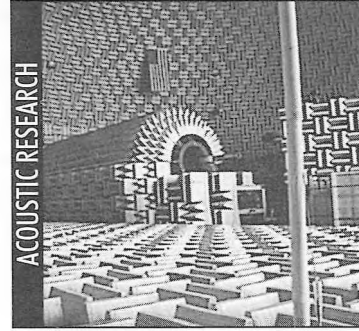


AUDIOMETRIC ROOMS & SUITES

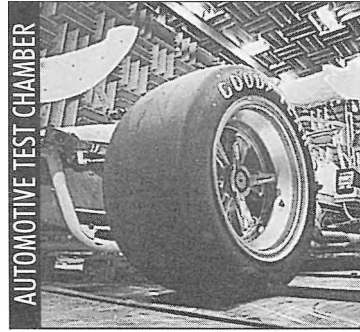
SOUND SOLUTIONS FOR THE FUTURE



ARCHITECTURAL ACOUSTICS



ACOUSTIC RESEARCH



AUTOMOTIVE TEST CHAMBER



REVERBERATION ROOM

# ECKEL

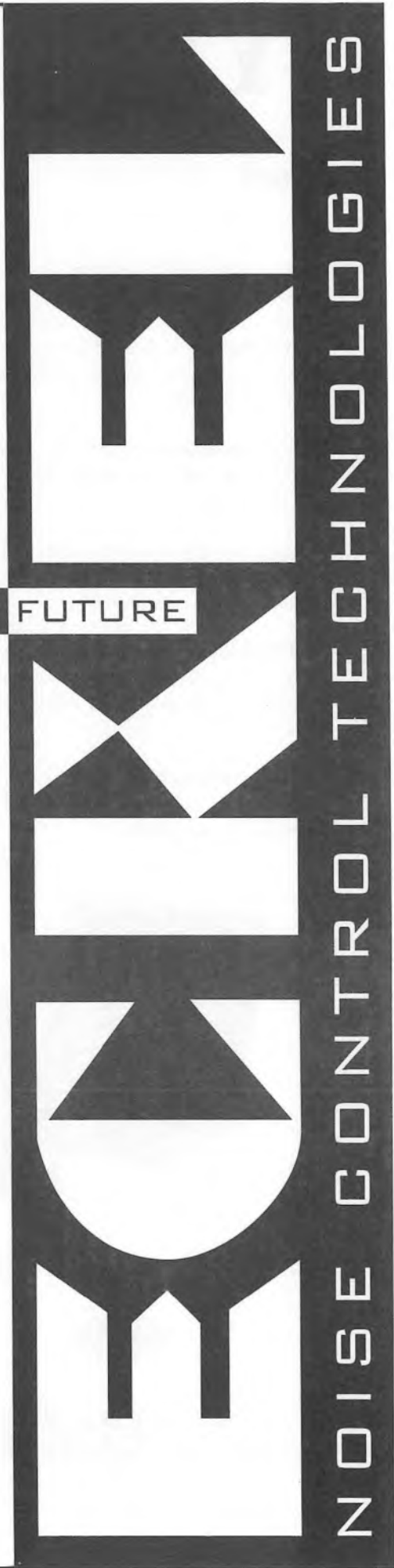
NOISE CONTROL TECHNOLOGIES

CANADIAN OFFICE

Box 776 100 Allison Avenue Morrisburg ON K0C 1X0

Tel: 613-543-2967 800-563-3574 Fax: 613-543-4173

Web site: [www.eckel.ca/eckel](http://www.eckel.ca/eckel) e-mail: [eckel@eckel.ca](mailto:eckel@eckel.ca)



# SYSTEM 824

SLM/RTA

Five sophisticated acoustical instruments  
in One!

**1 Integrating Sound Level Meter** meeting Type 1 Standards with simultaneous measurement of sound pressure levels using fast, slow, and impulse detector, and simultaneous A, C, and flat weighting. It measures 48 sound pressure parameters at once! All this with a 105 dB linearity range!

**Simple Sound Analyzer** with simultaneous sound pressure level measurement and real-time 1/3 octave frequency analysis.

**Logging Sound Level Meter** permits data gathering of broadband sound pressure levels and frequency spectra over user-defined time intervals.

**Real Time Frequency Analyzer** with 1/1 and 1/3 octave analysis over a 20kHz frequency range and optimized for characterizing steady-state or high speed transient events.

**Fast Fourier Transform Analyzer** with 100, 200, and 400 lines resolution and 20kHz range for specific frequency investigations.



Listen  with Larson•Davis



For use in a wide variety of applications



#### Research and Development

- Building Acoustics
- Sound Power Determination
- Vibration measurements
- Statistics
- Simple Point Shoot
- Transient Capture



#### Environmental

- Aircraft Noise
- Industrial Noise
- General Surveys
- Transportation Noise
- Community Noise



#### Worker Safety

- Noise Exposure Measurements
- Work Place Surveys
- Machinery Noise
- Audiometric Calibration
- Simultaneous C minus A Measurements

**Dalimar**

**Instruments Inc.**

*At your service*  
since 1986

193, Joseph Carrier, Vaudreuil-Dorion, Quebec, Canada J7V 5V5 Tel.: (450) 424-0033 Fax: (450) 424-0030  
1234 Reid Street, Suite 8, Richmond Hill, Ontario, Canada L4B 1C1 Tel.: (905) 707-9000 Fax: (905) 707-5333  
E-mail: info@dalimar.ca Website: www.dalimar.ca

# NOISE AND VIBRATION

## WANT MORE CONFIDENCE IN YOUR MEASUREMENTS?

**PORTABLE ANALYZERS 2-32 CHANNELS**

- FFT
- Recorder
- Octave
- Order Tracking
- Real-Time & Off-Line

**OR38      OR25      OR24**

- Data management, report generation
- ODS, Modal
- Sound Intensity
- Sound Power
- Balancing
- Vibration Diagnostic

## THEN ASK FOR THE COMPLETE RANGE OF OROS ANALYZERS & SOLUTIONS

• Need a complete solution, guaranteed by a recognized name in the NV field? Just choose an OR24, OR25 or OR38 analyzer and select the application package you need.

• Think you may need more in the future? With the OROS range, you can expand your hardware as well as add software modules at any time.

• Can't take the time to repeat your tests? The new OR38 records the original time domain data on the internal disk from 1 to 32 channels, and can also run several analyzers simultaneously. This unprecedented flexibility also ensures never losing your data.

OROS Analyzers and Solutions cover a wide range of measurement needs in the noise and vibration field. For structural, rotating as well as acoustics measurements, OROS offers complete solutions.

	Channels	Frequency band	Interface	Calculation	Recording	Power	Weight
OR24	2, 4	20kHz	PCMCIA	DSP	PC disk	AC, external DC-Batt	2kg
OR25	2, 4, 8, 16	20kHz	PCMCIA	DSP	PC disk	AC, DC, Batt	5kg
OR38	8, 16, 24, 32	40kHz	LAN	DSP or PC	Internal or PC disk	AC, DC, Batt	7kg

design by genco oil - france: +33 475 982 999

# Dalimar

## Instruments Inc.

by OROS

*1 year service*  
since **1986**

Montreal : Tel. : (450) 424-0033 Fax : (450) 424-0030    Toronto : Tel. : (905) 707-9000 Fax : (905) 707-5333  
**E-mail: info@dalimar.ca    WEBSITE: WWW.DALIMAR.CA**